Threshold behavior and electro-optical properties of twisted nematic layers with weak anchoring in the tilt and twist angle

R. Hirning, W. Funk, and H.-R. Trebin
Institut für Theoretische und Angewandte Physik der Universität Stuttgart, Pfaffenwaldring 57, W-7000 Stuttgart 80, Federal Republic of Germany

M. Schmidt and H. Schmiedel
Sektion Physik der Universität Leipzig, Linnéstr. 5, O-7010 Leipzig, Federal Republic of Germany

(Received 27 March 1991; accepted for publication 9 July 1991)

Analytical and numerical calculations of threshold behavior and electro-optical characteristics in twisted chiral nematic layers are presented, when weak anchoring in the tilt *and* twist angle of the director is assumed. An analytical expression for the effective twist angle and the Fréedericksz threshold voltage is derived. In cells with bistabilities, we investigate the influence of the anchoring parameters and device parameters on the width of the hysteresis. Using the 4×4-matrix formalism of Berreman [J. Opt. Soc. Am. **62**, 502 (1972)], we demonstrate the influence of the weak anchoring on the transmission-versus-voltage characteristic.

I. INTRODUCTION

The director configuration in twisted nematic layers like TN,[1] OMI,[2] or SBE[3] cells is determined by the following three major features: First, the elastic forces in the liquid crystal, described by the well-known Frank–Oseen–Zocher free-energy density[4]; second, the influence of an external applied voltage modeled through an electric energy term of the form $\frac{1}{2}\mathbf{DE}$, where $\mathbf{D}$ is the displacement vector and $\mathbf{E}$ the internal electric field vector; and third, the anchoring of the director at the substrate boundaries of the layer. Earlier work in analytical and numerical calculations used either strong[5,6] or weak[7–9] anchoring in the tilt angle of the director (polar anchoring), i.e., its orientation with respect to the surface *normal* is either fixed or can vary with the applied voltage. Several authors report theoretical and experimental results[10,11] on weak anchoring effects only in the twist angle (azimuthal anchoring), where the director is parallel to the surface but is allowed to leave its preferred orientation with respect to an axis *in* the surface (easy axis) under the influence of an applied voltage. This axis can be realized, for instance, by rubbing the surface carefully in one direction. Recently, some experimental studies of both types of anchoring have been published,[12–14] showing that typical values of the anchoring energy are in the range 10^{-6}–10^{-5} N/m for homeotropically anchored nematics and 10^{-6}–10^{-3} N/m for planarly oriented nematics. In the last case, the azimuthal anchoring energy is one order of magnitude smaller than the polar energy. As far as we know, only the simulation program DIMOS[15] incorporates both types of anchoring.

In this paper the two kinds of anchoring are combined and studies are presented of the influence on the Fréedericksz threshold voltage, on the hysteresis width, and on the optical properties in such cells.

II. THEORY

We consider a nematic cell of thickness d located between the planes $z=0$ and $z=d$ of a Cartesian coordinate system and mirror symmetric with respect to the middle plane $z=d/2$. The director $\mathbf{n}$ is described by the tilt angle θ (measured from the layer normal) and the twist angle φ. The dielectric constants parallel and perpendicular to the director are denoted by $\varepsilon_\parallel$ and $\varepsilon_\perp$, and we assume $\Delta\varepsilon = \varepsilon_\parallel - \varepsilon_\perp > 0$. The elastic constants for splay, twist, and bend are denoted by k_{11}, k_{22}, and k_{33}, respectively. The pitch of the material induced through a chiral dopant is named p_0.

Using the abbreviations

$$\begin{aligned} a_1 &= k_{33}\cos^2\theta + k_{11}\sin^2\theta, \\ a_2 &= (k_{33}\cos^2\theta + k_{22}\sin^2\theta)\sin^2\theta, \\ a_3 &= (2\pi/p_0)k_{22}\sin^2\theta, \\ a_4 &= \varepsilon_0(\varepsilon_\perp + \Delta\varepsilon\cos^2\theta) \end{aligned} \tag{1}$$

(ε_0 is the dielectric constant in vacuum), the free-energy density in the bulk can be written as[4]

$$f_B = \tfrac{1}{2}a_1\theta'^2 + \tfrac{1}{2}a_2\varphi'^2 - a_3\varphi' - \tfrac{1}{2}a_4\Phi'^2, \tag{2}$$

where the prime indicates differentiation with respect to z and where Φ is the electric potential inside the layer. Note that the last term represents the electric contribution $\frac{1}{2}\mathbf{DE}$, when we assume a dielectric material law for uniaxial nematics in the form

$$D_i = (\varepsilon_\perp\delta_{ij} + \Delta\varepsilon n_i n_j)E_j, \tag{3}$$

with $E_j = -\partial_j\Phi$. Because we are interested in the director configuration for fixed voltage, we must add the electric contribution with the minus sign.[16]

The weak anchoring in the tilt and twist angle is described by a surface free-energy of the Rapini–Papoular type[17]:

$$\begin{aligned} F_S(z=0) &= \tfrac{1}{2}C_\theta\sin^2(\theta-\theta_p) + \tfrac{1}{2}C_\varphi\sin^2\varphi, \\ F_S(z=d) &= \tfrac{1}{2}C_\theta\sin^2(\theta-\theta_p) + \tfrac{1}{2}C_\varphi\sin^2(\varphi-\varphi_p) \end{aligned} \tag{4}$$

 0021-8979/91/084211-06$03.00

The factors C_θ and C_φ measure the anchoring strength in the tilt and twist angle, respectively, θ_p (pretilt) describes the preferred tilt of the director at the surface, and φ_p (pretwist) is the difference between the preferred orientation at the top and bottom surface in the twist angle. The influence of the surface is restricted to the place of the aligning substrate.

The total free energy per unit area of the cell is now given by

$$F=\int_0^d f_B\,dz+F_S(0)+F_S(d). \tag{5}$$

A. Fréedericksz threshold voltage (analytical)

In this section we restrict ourselves to the case where the pretilt is equal to 90°. First, we investigate the director configuration if no electrical voltage is applied. The Eulerian equations resulting from the condition that the first variation of F in Eq. (5) vanishes, split into the bulk equations and the surface torque balances. The bulk equations are given by

$$\begin{aligned}&(k_{11}\sin^2\theta+k_{33}\cos^2\theta)\theta''-(k_{33}-k_{11})\sin\theta\cos\theta\theta'^2\\&\quad-[k_{33}+2(k_{22}-k_{33})\sin^2\theta]\sin\theta\cos\theta\varphi'^2\\&\quad-(4\pi/p_0)k_{22}\sin\theta\cos\theta\varphi'=0\end{aligned} \tag{6}$$

and

$$\begin{aligned}&(k_{33}\cos^2\theta+k_{22}\sin^2\theta)\sin^2\theta\varphi'-(2\pi/p_0)k_{22}\sin^2\theta\\&\quad=\text{const.}\end{aligned} \tag{7}$$

The surface torque balances for tilt and twist, respectively, are given by

$$\left.\frac{\partial f_B}{\partial\theta'}\right|_{z=0}=C_\theta\sin(\theta-\theta_p)\cos(\theta-\theta_p) \tag{8}$$

and

$$\left.\frac{\partial f_B}{\partial\varphi'}\right|_{z=0}=C_\varphi\sin\varphi\cos\varphi. \tag{9}$$

Corresponding equations hold for $z=d$. Equations (6) and (7) are solved by the distribution $\theta(z)=90°$, $\varphi'(z)=\text{const}$. Hence the director is planar and uniformly twisted with

$$\varphi(z)=\varphi_0+(z/d)\varphi_{\text{eff}}, \tag{10}$$

where the effective total twist angle is given by

$$\varphi_{\text{eff}}=\varphi_p-2\varphi_0, \tag{11}$$

and $\varphi_0=\varphi(0)$ is calculated from Eq. (9).

Let us discuss the influence of the weak coupling in the twist. We first note that the deviation angle from the pretwist direction, φ_0, vanishes if the pitch due to the chiral additive matches the pretwist given by the surface treatment, i.e., $\varphi_p=2\pi d/p_0$. Therefore, the effective twist in this case is equal to the pretwist and weak twist coupling does not affect the director distribution for zero voltage. However, if $\varphi_p>2\pi d/p_0$, the effective twist becomes smaller than the pretwist, $\varphi_{\text{eff}}<\varphi_p$, and vice versa. For strong twist anchoring we obtain $\varphi_{\text{eff}}=\varphi_p$.

To calculate the Fréedericksz threshold we modify the ansatz used for small deformations in the case of strong tilt and twist anchoring[18]:

$$\theta(z)=\theta_m\sin[\pi z/(d+2b)], \tag{12}$$

where θ_m denotes the midplane tilt angle and b is a fictive extrapolation length to describe the weak tilt anchoring. Substituting Eqs. (12) and (10) into f_B and integrating over the cell thickness yields the free energy as a function of θ_m and φ_0. The equations of the variational principle are then solved in the limit $\theta_m\to 90°$, which leads to the Fréedericksz threshold voltage V_F at which the deformation starts.[18] We obtain

$$V_F=\sqrt{\frac{k_{11}\pi^2R^2+\varphi_{\text{eff}}[\varphi_{\text{eff}}(k_{33}-2k_{22})+4k_{22}\pi d/p_0]}{\varepsilon_0(\varepsilon_\parallel-\varepsilon_\perp)}}, \tag{13}$$

where φ_{eff} is determined by Eq. (11), φ_0 and R are the solutions of the transcendental equations,

$$\varphi_p-2\varphi_0-\frac{2\pi d}{p_0}=\frac{C_\varphi d}{k_{22}}\sin\varphi_0\cos\varphi_0 \tag{14}$$

and

$$\cot\left(\frac{\pi R}{2}\right)=\pi R\,\frac{k_{11}}{C_\theta d}. \tag{15}$$

Note that Eq. (13) involves weak anchoring for both the tilt and twist. For the case of strong twist anchoring we obtain the same result as Becker *et al.*,[6] who expanded the corresponding differential equations to calculate V_F.

Finally, we remark that the Fréedericksz threshold voltage is affected by weak twist coupling only if the pitch does not match the pretwist. The weak twist anchoring can then increase or decrease the Fréedericksz threshold voltage depending on the ratios $(2\pi d/p_0)/\varphi_p$ and k_{33}/k_{22}. In contrast to this behavior, a weak tilt coupling always decreases V_F as was already mentioned by Becker *et al.*[6]

B. Numerical procedure

The first step in the calculation of optical properties consists of the determination of the director configuration. To this end, we transform the Euler–Lagrange equations resulting from the extremalization of the bulk free energy into a system of Hamilton equations by performing a Legendre transformation with respect to the variables θ, φ, and Φ:

$$\theta'=\frac{\partial f_B^L}{\partial T}=\frac{T}{a_1},$$

$$\varphi'=\frac{\partial f_B^L}{\partial P}=\frac{P+a_3}{a_2},$$

$$\Phi'=\frac{\partial f_B^L}{\partial U}=-\frac{U}{a_4},$$

$$T' = -\frac{\partial f_B^L}{\partial \theta} = \frac{b_1}{2a_1^2} T^2 - \frac{b_3}{a_2}(P + a_3) + \frac{b_2}{2a_2^2}(P + a_3)^2 - \frac{b_4}{2a_4^2} U^2,$$

$$P' = -\frac{\partial f_B^L}{\partial \varphi} = 0, \tag{16}$$

$$U' = -\frac{\partial f_B^L}{\partial \Phi} = 0,$$

where f_B^L is the Legendre transform of f_B:

$$f_B^L(\theta, T, P, U) = \theta' T + \varphi' P + \Phi' U - f_B, \tag{17}$$

and $b_i = \partial a_i / \partial \theta$, $i = 1, 4$, and T, P, U are the conjugated momenta:

$$T = \frac{\partial f_B}{\partial \theta'} = a_1 \theta',$$

$$P = \frac{\partial f_B}{\partial \varphi'} = a_2 \varphi' - a_3, \tag{18}$$

$$U = \frac{\partial f_B}{\partial \Phi'} = -a_4 \Phi'.$$

As φ and Φ are cyclic variables, the corresponding momenta P and U represent integration constants for the problem, where U is equal to the z component of the displacement vector **D**. To these equations we have to add the boundary conditions (8) and (9), expressed in the new variables at $z = 0$:

$$T = +\frac{\partial F_S}{\partial \theta} = C_\theta \sin(\theta - \theta_p) \cos(\theta - \theta_p),$$

$$P = +\frac{\partial F_S}{\partial \varphi} = C_\varphi \sin \varphi \cos \varphi, \tag{19}$$

and at $z = d$:

$$T = -\frac{\partial F_S}{\partial \theta} = -C_\theta \sin(\theta - \theta_p) \cos(\theta - \theta_p),$$

$$P = -\frac{\partial F_S}{\partial \varphi} = -C_\varphi \sin(\varphi - \varphi_p) \cos(\varphi - \varphi_p). \tag{20}$$

Equations (16), (19), and (20) represent a nonlinear boundary-value problem, which we solve numerically by a multidimensional shooting method using standard library routines.

The second step is to solve the Maxwell equations inside the layer. For this problem we use the 4×4 formalism of Berreman.[19–21] To decide whether our numerical calculated optical transfer matrix of the nematic layer is correct, we use the condition[22] that the modulus of the determinant for this matrix must be equal to 1, which expresses the law of conservation of energy.

Our main emphasis was to implement an efficient code which works properly and fast over a broad range of material and device parameters. On an IBM PC/AT with 10 MHz, for instance, the calculation of an electro-optical characteristic needs about 10 min independent of the existence of bistabilities.

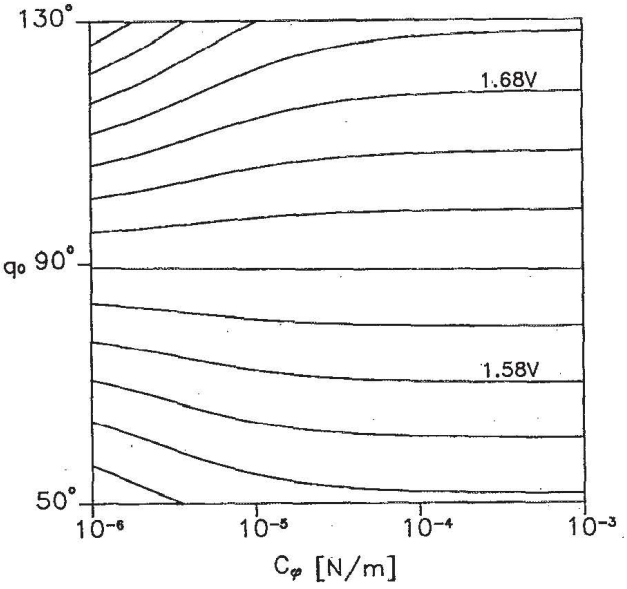

FIG. 1. Fréedericksz threshold voltage for a 90° TN cell as a function of C_φ and q_0. The difference between neighboring lines is 0.02 V. Material parameters are $k_{33}/k_{11} = 0.8$, $k_{22}/k_{11} = 0.45$, $\varepsilon_\parallel/\varepsilon_\perp = 2.3$; the cell thickness is 5.6 μm.

III. NUMERICAL RESULTS AND DISCUSSION

A. Fréedericksz threshold voltage (numerical)

To test the correctness of the analytical expression for the Fréedericksz threshold voltage, we have calculated it for a 90° TN cell with $q_0 = 2\pi d/p_0$ and C_φ as variables, $\theta_p = 90°$, and with fixed values of $C_\theta = 10^{-4}$ N/m. Figure 1 shows the lines of constant threshold voltage resulting from our numerical calculations. (Note that we measure

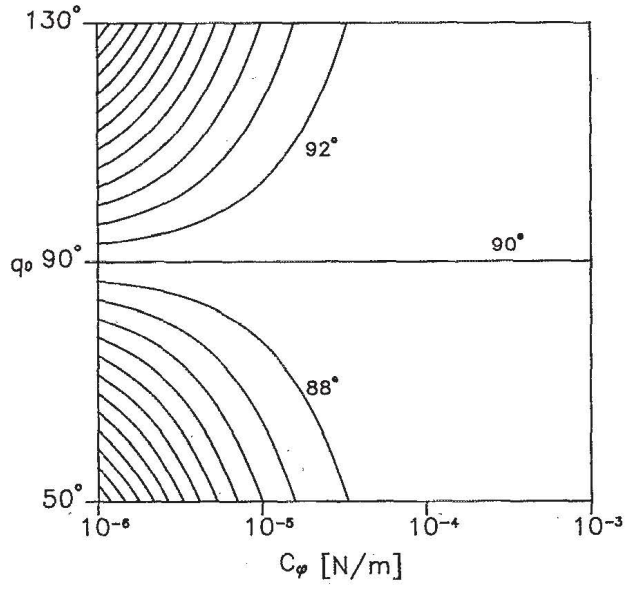

FIG. 2. Effective twist angle for a 90° TN cell as a function of C_φ and q_0. The difference between neighboring curves is 2°. Material parameters are as in Fig. 1.

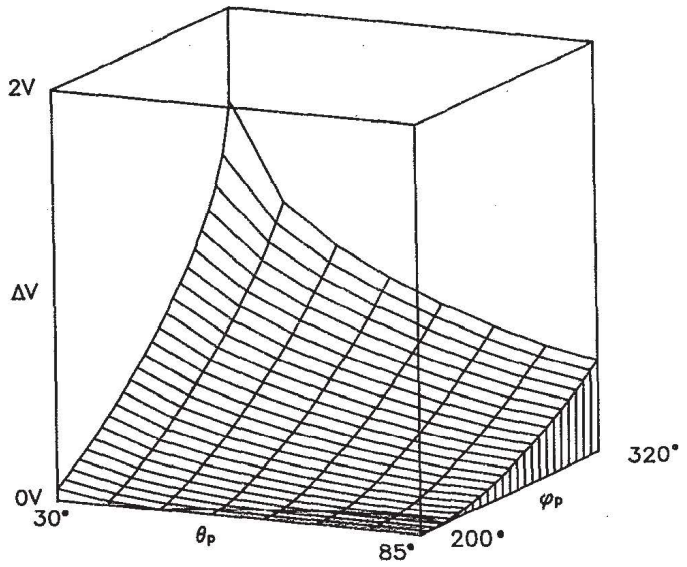

FIG. 3. Hysteresis width for a 240° STN cell as a function of φ_p and θ_p; the anchoring strength C_φ is 10^{-4} N/m. Material parameters are $k_{33}/k_{11} = 2.1$, $k_{22}/k_{11} = 0.4$, $\varepsilon_\parallel/\varepsilon_\perp = 2.0$; the cell thickness is 5.6 μm.

q_0 in rad, e.g., $q_0 = 90°$ means that the intrinsic pitch is identical with the extrinsic pitch imposed by the boundary conditions.) The values of V_F resulting from the analytical calculations [see Eq. (13)] are identical with the numerical ones and show the behavior predicted in Sec. II A.

B. Effective twist angle

In Fig. 2 we give the curves of constant effective twist angle φ_{eff} at zero applied voltage V as a function of q_0 and C_φ resulting from our numerical calculations. It is seen that φ_{eff} increases with decreasing C_φ if q_0 is greater than the pretwist φ_p; on the other hand, if q_0 is smaller than the φ_p, φ_{eff} is decreasing with decreasing C_φ. Analogously to

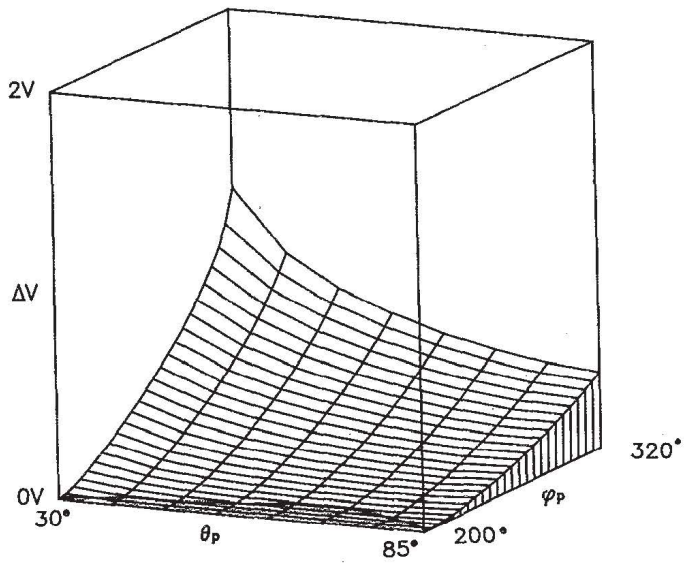

FIG. 4. Same plot as in Fig. 3 with $C_\varphi = 10^{-5}$ N/m.

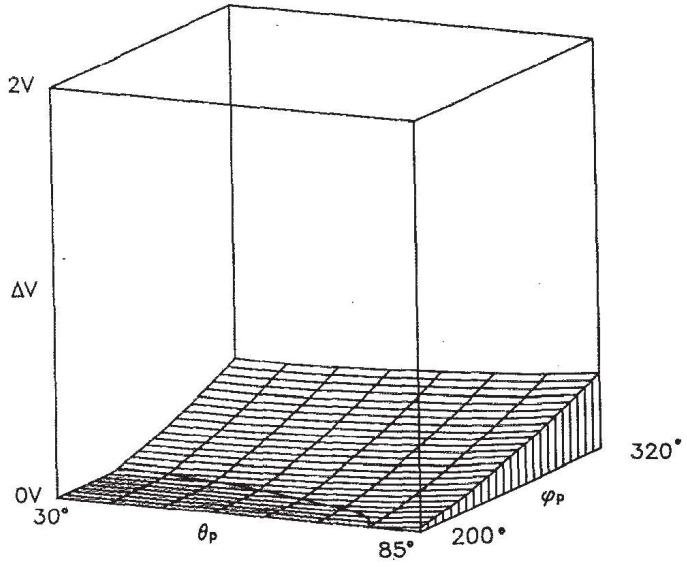

FIG. 5. Same plot as in Fig. 3 with $C_\varphi = 10^{-6}$ N/m.

the preceding section the analytical values [resulting from Eqs. (11) and (14)] agree with the numerical ones.

C. Width of the hysteresis

In highly twisted cells with nonzero pretilt, there is the possibility of bistable director configurations,[8,18,23–27] which becomes evident by a hysteresis in the θ_m-versus-voltage curve. In Figs. 3–5, we have plotted the width of the hysteresis ΔV as a function of θ_p and φ_p for $C_\varphi = 10^{-4}$, 10^{-5}, and 10^{-6} N/m. C_θ was held constant at 10^{-4} N/m, and we have chosen q_0 equal to φ_p. We get a

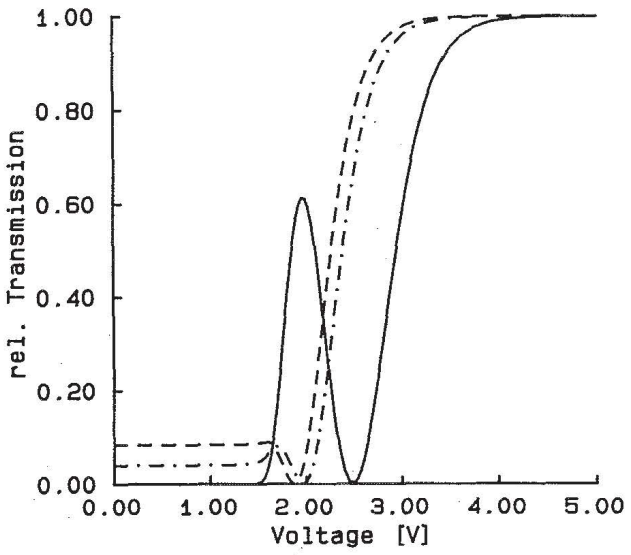

FIG. 6. Transmission-vs-voltage characteristic for a 90° TN cell of thickness $d = 5.6$ μm; the material parameters are the same as in Fig. 1; the optical birefringence indices are $n_o = 1.5$ and $n_e = 1.65$, the wavelength λ is 550 nm, polarizer and analyzer are parallel to the preferred direction in the twist angle at $z = 0$; the solid line represents the curve for $C_\varphi = 10^{-6}$ N/m, the dashed-dotted line for $C_\varphi = 10^{-5}$ N/m, and the dashed line for $C_\varphi = 10^{-4}$ N/m; C_θ is 10^{-4} N/m in each case.

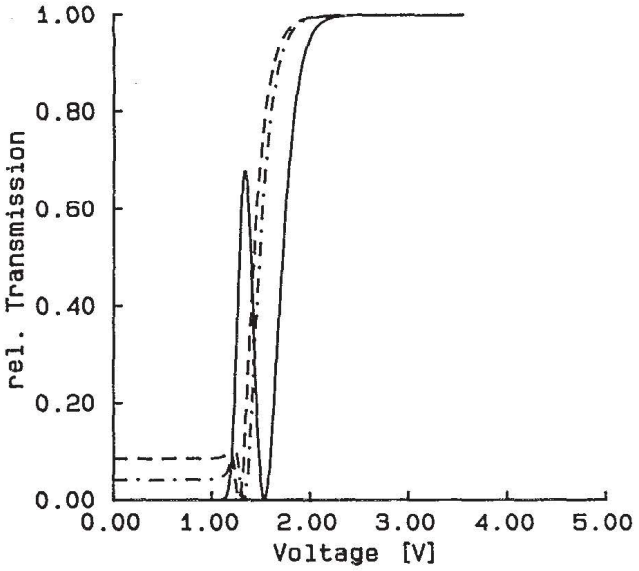

FIG. 7. Same curves as in Fig. 6 with $C_\theta = 10^{-5}$ N/m.

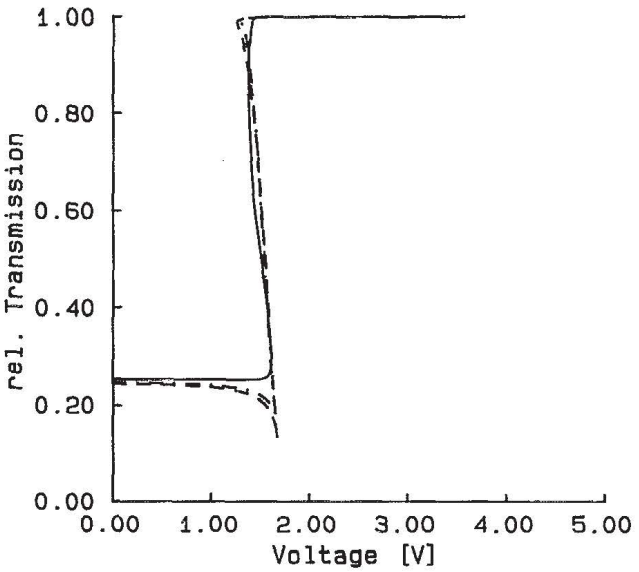

FIG. 9. Same curves as in Fig. 8 with $C_\theta = 10^{-5}$ N/m.

monotonic increase of ΔV in the variable φ_p. Further, it can be seen that for fixed φ_p and θ_p the width of the hysteresis falls with decreasing C_φ. If C_φ gets smaller the onset of the hysteresis increases for φ_p and decreases for θ_p.

D. Transmission-versus-voltage curves

One of the most important features for a twisted nematic layer is its transmission-versus-voltage characteristic. In Figs. 6 and 7 we show these curves for a TN cell with $C_\theta = 10^{-4}$ N/m and $C_\theta = 10^{-5}$ N/m. The parameter of the curves is C_φ, the wave vector of the incident light with $\lambda = 550$ nm is normal to the cell surface, and we assume a pretilt θ_p of 89°. A characteristic property in both figures is the peak below the optical threshold voltage, which is defined as that voltage for which the Mauguin parameter M in the middle of the cell becomes greater than unity.[28] The peak appears at the voltage for which the voltage-dependent optical path difference $\overline{\Delta nd}$ averaged over the whole cell causes a constructive interference of the extraordinary and ordinary optical normal modes. This proves that the peak is a birefringence effect. Our calculations show further that the height of the peak is raised by reducing C_φ, whereas the width is getting broader for increasing C_θ. The wavelength λ of the incident light influences the peak, too; with increasing λ the height increases slightly, the location is slightly shifted to smaller voltages, whereas the shape remains almost unchanged.

Figures 8 and 9 show the same curves as in Figs. 6 and 7 but now for a cell with a pretilt of 70°, a pretwist φ_p of 240°, and light of $\lambda = 589$ nm. We have chosen the optical path difference in such a way that the cell works in the SBE mode. It is seen that a weak anchoring in the twist reduces the hysteresis (see the preceding section), whereas a weak anchoring in the tilt enhances it.

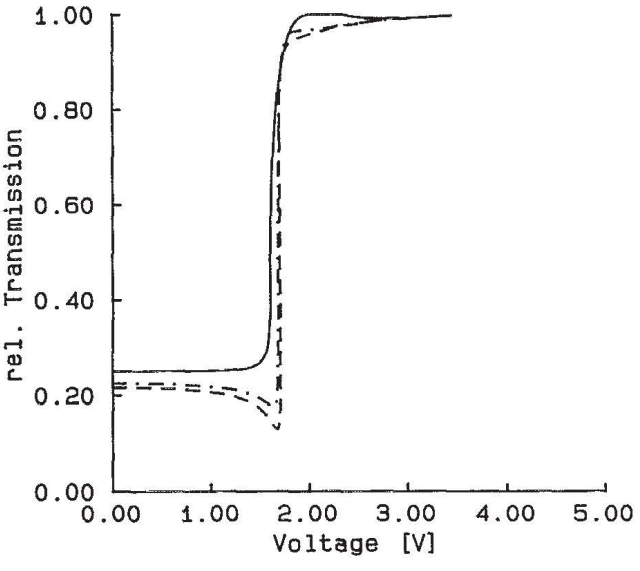

FIG. 8. Transmission-vs-voltage characteristic for a 240° SBE cell of thickness $d = 5.6$ μm; the material parameters are the same as in Fig. 3; the optical birefringence indices are $n_o = 1.49$ and $n_e = 1.63$, the wavelength λ is 589 nm, polarizer and analyzer are oriented parallel exactly in the middle between the preferred directions in the twist angle at $z = 0$ and $z = d$; the solid line represents the curve for $C_\varphi = 10^{-6}$ N/m, the dashed-dotted line for $C_\varphi = 10^{-5}$ N/m, and the dashed line for $C_\varphi = 10^{-4}$ N/m; C_θ is 10^{-4} N/m in each case.

[1] M. Schadt and W. Helfrich, Appl. Phys. Lett. **18**, 127 (1971).
[2] M. Schadt and F. Leenhouts, Appl. Phys. Lett. **50**, 236 (1987).
[3] T. J. Scheffer and J. Nehring, J. Appl. Phys. **58**, 3022 (1985).
[4] P. G. de Gennes, *The Physics of Liquid Crystals* (Clarendon, Oxford, 1974).
[5] G. Baur, F. Windscheid, and D. Berreman, Appl. Phys. **8**, 101 (1975).
[6] M. E. Becker, J. Nehring, and T. J. Scheffer, J. Appl. Phys. **57**, 4539 (1985).
[7] J. Nehring, A. Kmetz, and T. J. Scheffer, J. Appl. Phys. **47**, 850 (1976).
[8] H. A. van Sprang and P. A. Breddels, J. Appl. Phys. **60**, 968 (1986).
[9] G. Haas, H. Wöhler, M. Fritsch, and D. Mlyinski, 17. Freiburger Arbeitstagung Flüssigkristalle, 1987.
[10] G. Barbero, E. Miraldi, C. Oldano, M. L. Rastello, and P. Taverna Valabrega, J. Phys. (Paris) **47**, 1411 (1986).
[11] S. Faetti, M. Gatti, V. Palleschi, and T. J. Sluckin, Phys. Rev. Lett. **55**, 1681 (1985).
[12] T. Sugiyama, S. Kuniyasu, and D. Seo, Jpn. J. Appl. Phys. **29**, 2045 (1990).

[13] K. Ogawa, N. Mino, and K. Nakajima, Jpn. J. Appl. Phys. **29**, L1689 (1990).
[14] M. Blinov, A. Kabayenkov, and A. Sonin, Liq. Cryst. **5**, 645 (1989).
[15] M. Becker, Electronic Displays, Wiesbaden, 1988.
[16] R. Thurston and D. Berreman, J. Appl. Phys. **52**, 508 (1981).
[17] A. Rapini and M. Papoular, J. Phys. (Paris) Colloq. **30**, C4-54 (1969).
[18] M. Schmidt and H. Schmiedel, Mol. Cryst. Liq. Cryst. **167**, 89 (1989).
[19] D. W. Berreman, J. Opt. Soc. Am. **62**, 502 (1972).
[20] K. Eidner, G. Mayer, M. Schmidt, and H. Schmiedel, Mol. Cryst. Liq. Cryst. **172**, 191 (1989).
[21] H. Wöhler, G. Haas, M. Fritsch, and D. Mlynski, J. Opt. Soc. Am. A **5**, 1554 (1988).
[22] M. Schmidt and H. Schmiedel, Mol. Cryst. Liq. Cryst. **172**, 223 (1989).
[23] S. Saito, M. Kamihara, and S. Kobayashi, Mol. Cryst. Liq. Cryst. **139**, 171 (1986).
[24] T. J. Scheffer and J. Nehring, Appl. Phys. Lett. **45**, 1021 (1984).
[25] D. W. Berreman and W. R. Heffner, J. Appl. Phys. **52**, 3032 (1981).
[26] H. K. Singh, S. C. Jain, and S. Chandra, Liq. Cryst. **5**, 1373 (1989).
[27] E. P. Raynes, Mol. Cryst. Liq. Cryst. Lett. **4**, 1 (1986).
[28] C. Van Doorn and J. Heldens, Phys. Lett. **47A**, 135 (1974).